Application of LDV Profile Sensor Technology for Velocity Determination in Small Axial Gaps

C. Strauch[1,*], J. Peter[1], M. Dues[2], P U. Thamsen[1]
1: Chair of Fluid System Dynamics, Technische Universität Berlin, Germany
2: ILA R&D GmbH, Germany
* Correspondent author: carsten.strauch@tu-berlin.de

Keywords: Laser Doppler Velocimetry (LDV), LDV Profile-Sensor (LDV-PS), Ventricular Assist Device (VAD), Gap Flow Topology

ABSTRACT

In development of Ventricular Assist Devices (VADs), Computational Fluid Dynamics (CFD) have arise as a powerful tool to gain insights on flow topologies within rotary blood pumps. Information regarding flow patterns and shear-stress distributions is of enormous importance, since flow induced blood damage as well as platelet activation is attributed to shear rates. Although methods for verification of numerical results are available, a lack of experimental validation is recognizable. To enable an experimental validation (i) hydraulic properties as well as flow patterns need to be preserved and (ii) a non-intrusive optical measurement technique needs to be capable of resolving flow topologies appearing in rotary blood pumps. In this paper references to address (i) are provided and the focus is placed on (ii) by presenting a methodology to resolve flow topologies by usage of LDV Profile Sensor technology. This paper serves as a feasibility study and represents a preliminary stage towards actual optical measurements with rotary blood pumps. Therefore, a test bench with facilitated optical accessibility compared to Ventricular Assist Devices as well as operating conditions are introduced. Increased attention is dedicated to evaluation of measurement data by means of choosing a suitable procedure. Therefore, commonly used 2D-histograms for LDV raw data evaluation are compared to the method of Gaussian Kernel Density Estimation (Gaussian KDE). Subsequently, pre-processed raw data is further evaluated with a specially tailored Velocity Profile Validation Algorithm and determined circumferential velocity profiles are discussed. In summary, herein presented feasibility study is deemed successful and LDV Profile Sensor technology is capable of resolving flow topologies within small gaps as they appear in Ventricular Assist Devices. Thus, LDV Profile Sensor technology may improve development of rotary blood pumps.

1 Introduction

Investigation of velocity profiles between rotating and stationary disks has been part of research for a long period of time since flow topology is significantly responsible for frictional resistance and torque of the rotating disk. In (Schultz-Grunow, 1935) from 1935 experimental results on a disk with $D = 401.5\,mm$ ($R = 200.75\,mm$) and a gap width of $w = 4.0\,mm$ ($w/R = 0.0199$) are presented. Conclusions about the underlying velocity profile between stationary and rotating surfaces are drawn from measured torques by using the Navier-Stokes equations. In 1960, Daily and

Nece (Daily, 1960) extended experiments presented in (Schultz-Grunow, 1935) using a modular experimental setup to change the gap width ($D = 498.5\,mm$, $w = 6.3\,mm$ to $108.2\,mm$, $w/R = 0.0127$ to 0.217). Four characteristic flow regimes were defined (Regime I: laminar flow and merged boundary layers, Regime II: laminar flow and separate boundary layers, Regime III: turbulent flow and merged boundary layers, Regime IV: turbulent flow and separate boundary layers). Velocities were measured intrusively with a 2-hole cobra probe. With decreasing gap width s, intrusive measurements are no longer usable due to its excessive influence on the velocity profile. Therefore, laser-optical measurement techniques such as Laser Doppler Velocimetry (LDV) and Particle Image Velocimetry (PIV) have become widely used to investigate flow topology (Launder, 2009) (Haddadi, 2008). However, LDV technology reaches its limits as the length of measurement volume (MV) is of similar size as the gap to be measured. Within the measurement volume, spatial resolution of flow patterns is not possible.

In this paper, a novel LDV Profile Sensor-Technology is presented, which offers a high local resolution (10µm) within measurement volume and thus capability to investigate flow patterns in small gaps without interfering. A detailed description of LDV Profile Sensor and its working principle is provided in (Czarkse, 2002). Briefly, measurement volumes of two different wavelengths ($\lambda = 532\,nm$ and $\lambda = 561\,nm$) overlap. One offers a divergent fringe system and the other a convergent fringe system. The ratio of both detected Doppler frequencies is used to calculate position of particles inside the measuring volume.

Using the example of a gap size of s=0.5 mm, feasibility to measure a circumferential velocity profile between a rotating and stationary disk is demonstrated. Gaps of this size are commonly found in turbomachines and have technically relevant applications in various industrial fields, for example in designing wet clutches (Kriegeis, 2016).

The gap's characteristic shape in turbomachines has a great influence on hydraulic loss distributions. Therefore, investigation of flow topologies has been part of various studies (e.g., (Kosyna, 1992) (Florjancic, 1990) (Hamkins, 2000) (Lauer, 1997)).

Especially in biomedical engineering, there is a particular need for further investigations. Ventricular Assist Devices (VADs) are utilized when a patient's heart provides insufficient pumping power to supply the body with nutrients autonomously. In case of rotary blood pumps, devices are implanted and operate internally. Due to extremely limited available installation space, VADs are designed to be very small, resulting in unique engineering challenges during pump development. Reduction and prevention of shear-induced blood damage as well as platelet activation is of paramount importance. According to current state-of-the-art, shear stresses in fluid flow topologies are responsible for damaging blood components. Due to significantly different dimensions of rotary blood pumps compared to industrially deployed fluid flow machines, distribution of

hydraulic power and hydraulic losses as well as decomposition of hydraulic losses itself shift drastically. Thus, application of commonly used design guidelines for turbomachinery is not applicable for VADs. Consequently, Computational Fluid Dynamics (CFD) have emerged as the most common tool to support the developing process of Ventricular Assist Devices. Although, different methodologies exist to verify numerical calculations, reliable experimental validations are required and still missing. So far, only few studies on optical validations of flow topologies in rotary blood pump have been performed (Schüle, 2016) (Schüle, 2017) (Thamsen, 2019). This is attributed to hindered optical accessibility caused by commonly used design concepts for VADs, as shown in Fig. 1.

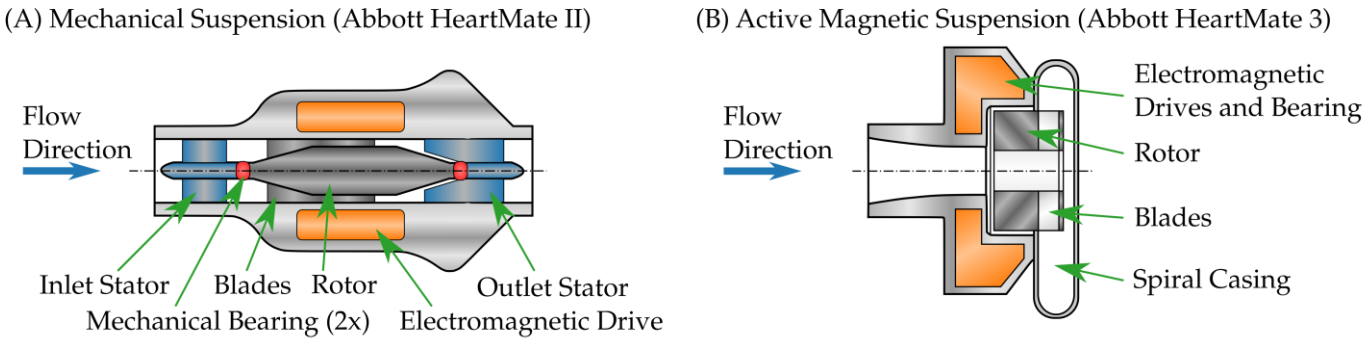

Fig. 1: Design concepts for rotary blood pumps and hindered optical accessibility. (A) Abbott HeartMate II with mechanical suspension and electromagnetic drive, (B) Abbott HeartMate 3 with active magnetic suspension and electromagnetic drive

Rotary blood pumps are usually mechanically suspended or magnetically levitated as well as electromagnetically driven. Therefore, either optical accessibility is hindered by drive parts or pump functionality is affected. Furthermore, reliable conclusions regarding hydraulic power and hydraulic losses becoming impaired. A methodology to carry out detailed hydraulic and mechanical measurements as well as to enable an optical accessibility for optical measurements whilst preserving hydraulic characteristics and dominant flow topologies is provided in (Strauch, 2020) (Strauch, 2021) (Strauch, 2022). This allows validation of flow patterns by optical measurements. Goal of this paper is to verify the feasibility of LDV Profile Sensor technology to resolve velocity profiles within small gaps as a new methodology for assisting development of rotary blood pumps.

The results presented here serve as a feasibility study for measuring flow within Ventricular Assist Devices by usage of LDV Profile Sensor technology.

2 Material and Methods

This part contains of four sub-chapters. First, a test bench is introduced which features an enhanced optical accessibility compared to Ventricular Assist Devices. Second, operating conditions as well as data acquisition settings are described. Third and fourth, a methodology is introduced on how extract velocity distributions from measured raw data and how to draw conclusions regarding velocity profiles.

2.1 Test Bench

Due to complex optical accessibility in ventricular assist devices, a test rig with favorable optical accessibility is developed for this feasibility study. In that test rig, a simplified flow is generated that has similarity to expected flow patterns between a rotating pump impeller and a stationary housing wall. Fig. 2 (A) shows the design of that test rig. In its left section the measurement chamber is located with a rotating glass disk D=50 mm (UV-VIS Coated, 1λ Fused Silica), which simulates the surface of a rotating impeller and is driven by an electric motor. Optical accessibility is realized by another stationary glass plate D=100 mm (MgF2 Coated, 1λ Fused Silica). A gap of s=0.5 mm is set between rotating and stationary disk via spacer pads (Fig. 2 (B) and (C)). The LDV Profile Sensor is positioned in front of this glass plate to measure circumferential velocities.

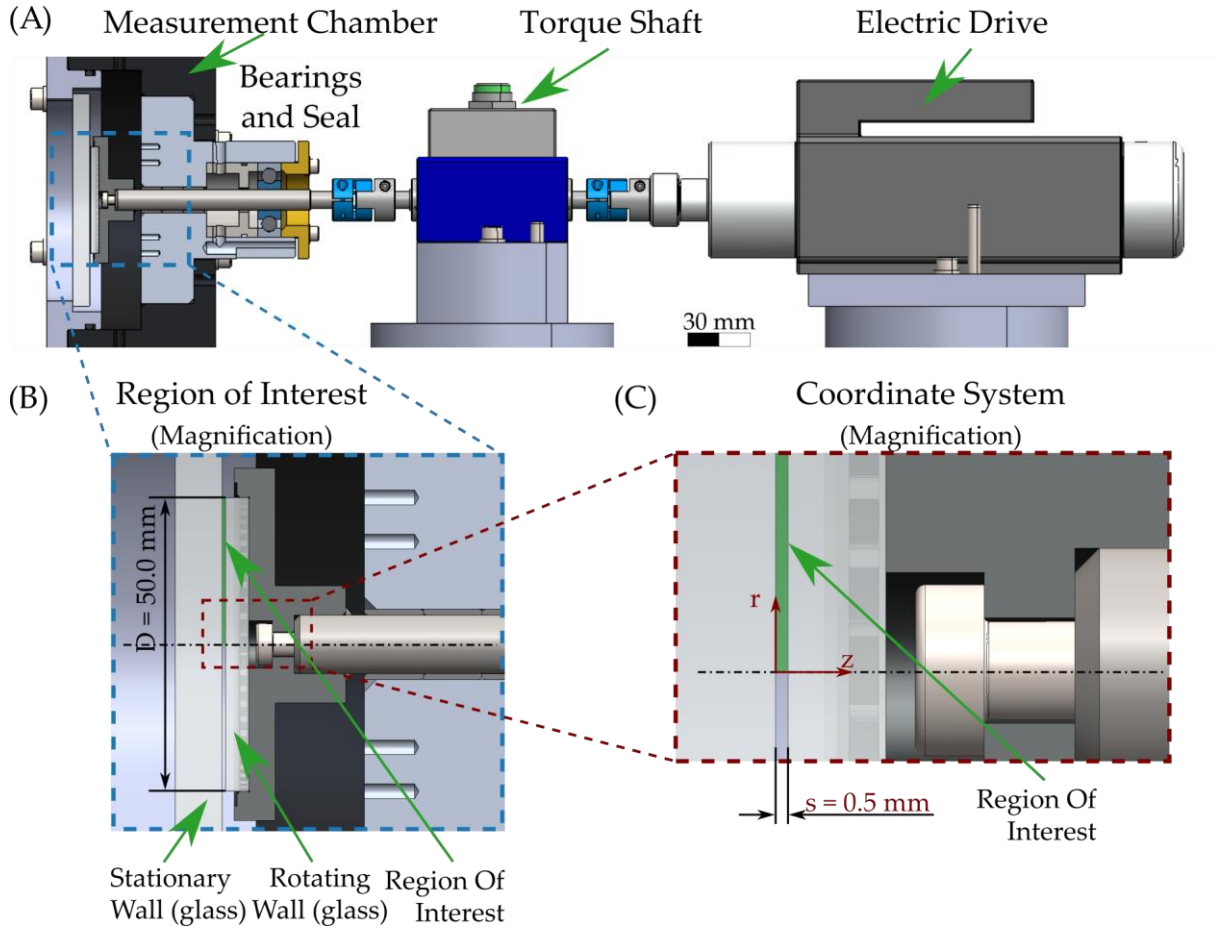

Fig. 2: (A) Test Bench, (B) Region of Interest, (C) and Coordinate System.

2.2 Operating Conditions and Data Acquisition

For a gap of size $s = 0.5\ mm$ circumferential velocity components c for five radii R are investigated at three rotational speeds n. Radii and rotational speeds are listed in Table 1. Chosen operating conditions lead in theory (e.g., (Schultz-Grunow, 1935) (Schubert, 1988) (Launder, 2009)) to (i) a linear velocity distribution at all five radii at $n = 1000\ min^{-1}$, (ii) a velocity distribution with well-defined core flow at $n = 3000\ min^{-1}$, and (iii) a rotational state where both (i) and (ii) co-exist at different radii ($n = 1500\ min^{-1}$). Water at $T = 22\ °C$ with added seeding particles is used for these studies. Data acquisition rates as well as axial positioning of measurement volume is described in Table 2 and visualized in Fig. 3 (A).

Length of measuring volume at a focal length of $L_f = 160\ mm$ in air amounts to $L_{MV} = 0.5\ mm$ and is stretched by refraction between air-glass and glass-water to $L_{MV} = 0.67\ mm$. Thus, measurement volume is longer than gap width to be investigated with $w = 0.5\ mm$, highlighting necessity of using LDV Profile Sensor Technology with a spatial resolution of 10 μm. Axial measurement positions shown in Table 2 and ratio of measurement volume to gap width are illustrated in Fig. 3 (A). Intensity of laser light within measuring volume is highest in the center, which indicates most particle detections to be expected at this position. For this reason, intensity maximum is set to three different axial positions to improve data acquisition rates. Fig. 3 (B) depicts an example of captured raw data for $R = 20.0\ mm$ at a speed of $n = 3000\ min^{-1}$. Raw data already allows to draw conclusions about the characteristic shape of investigated velocity profile. To determine exact velocity distribution $c(z)$, raw data must be evaluated in detail, which is addressed in the next chapter.

R	$n\ [min^{-1}]$		
$[mm]$	1000	1500	3000
10.0	linear	from linear to core flow	solid body core flow
12.5			
15.0			
17.5			
20.0			

Table 1: Operating conditions

ax. pos. $z\ [mm]$	0.00	0.20	0.40
No. of Data Points	25,000	50,000	50,000
max. acq. time $[s]$	4,000	2,400	2,400

Table 2: Data acquisition settings

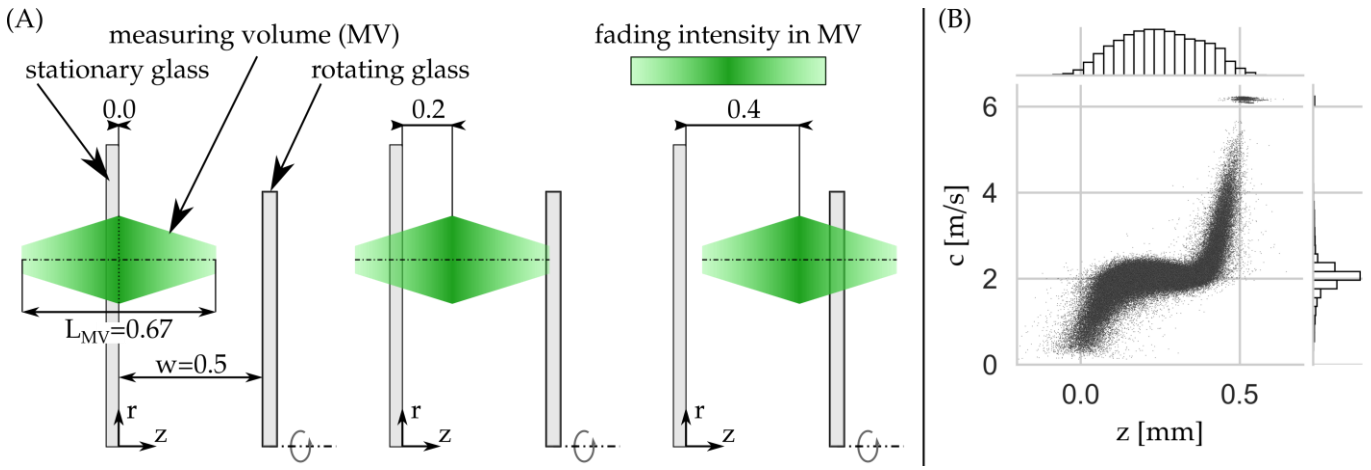

Fig. 3: (A) Dimensions of Measurement Volume (MV) in comparision to gap width w and axial measurement positions. MV's highest intesity is positioned at $z = 0.0$, $z = 0.2$, and $z = 0.4$ to improve data acquisition rates. (B) Measured raw data for a velocity profile at radius $R = 20.0\ mm$ and rotational speed $n = 3000\ min^{-1}$ with data distributions for z and c.

2.3 Evaluation of Measurement Data

As illustrated in Fig. 3 (B), turbulence in fluid flow creates a broad band of data points with clustered samples in a range of $(0.15 - 0.35)\ mm$ along z-axis and in a range of $(1.7 - 2.4)\ m/s$ along c-axis. To draw conclusions on velocity profile $c(z)$ and to characterize velocities in terms of their occurrences along the z-position, 2D histograms are widely used. Then, most frequent velocity at each z-position is used to reconstruct velocity profile. Fig. 4 illustrates the influence of discretization on data evaluation and drawing conclusions. With a low number of classes (Fig. 4 (A)), resolution is too coarse to draw reliable conclusions about the velocity profile $c(z)$. With an increasing number of classes, flow profile becomes more reliable (Fig. 4 (B)), but this pattern deteriorates when number of classes further increases (Fig. 4 (C) and (D)). In summary, choice of class width has an undesirable influence on the outcome and must be avoided.

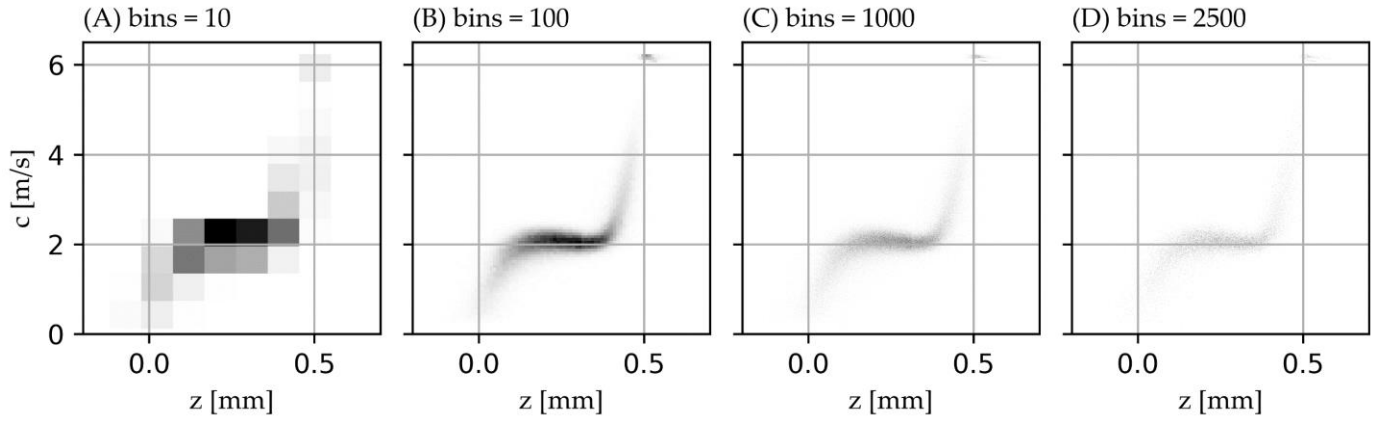

Fig. 4: Effect of number of classes in 2D-histograms on output value for (A) 10 bins, (B) 100 bins, (C) 1000 bins, and (D) 2500 bins, each in both axis directions

To eliminate influence of class width selection on final result, the method of "Gaussian Kernel Density Estimation (Gaussian KDE)" is applied instead of 2D histograms. Briefly explained, each data point is assigned an effective area in terms of a two-dimensional Gaussian distribution, so that neighboring data points are influenced by each other. Instead of a discretization, a continuous field is developed to prevent the influence of class widths. Gaussian KDE is exemplarily visualized in Fig. 5 for a one-dimensional case. Gaussian KDE is executed with a specially tailored python program using the SciPy open-source software with build-in function scipy.stats.gaussian_kde (The SciPy Community, 2022).

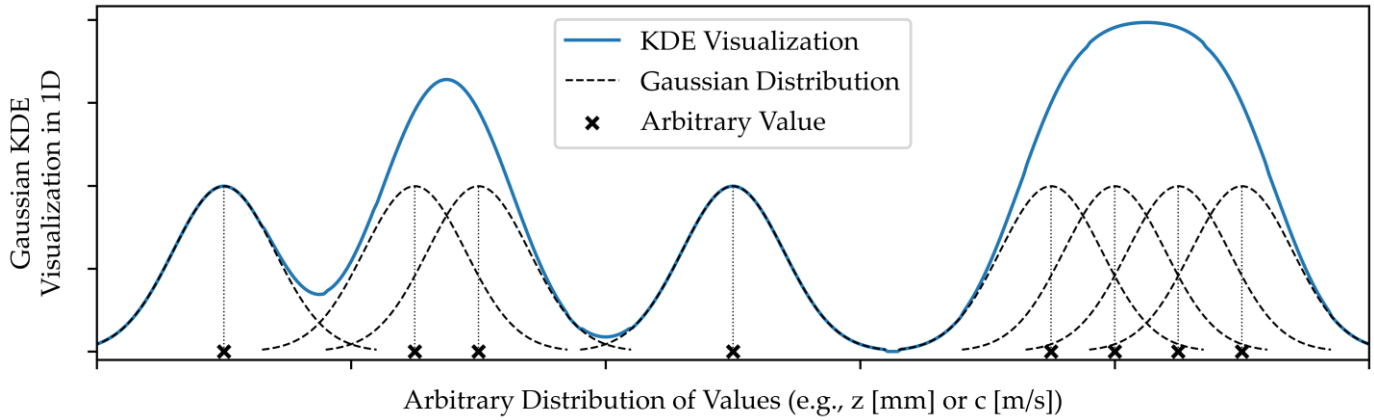

Fig. 5: Visualization of Gaussian Kernel Density Estimation (Gaussian KDE) for an arbitrarily distributed set of data. Each data point is assigned a gaussian distribution to influence neighboring data points and to develope a continuous density field.

Applying Gaussian KDE to raw data (Fig. 6 (A)) results in a continuous density distribution of measured data, which reveals underlying velocity profile (Fig. 6 (B)). To determine the velocity distribution $c(z)$ the Most Dense Points (MDP) along the z coordinate (Fig. 6 (C)) are further investigated. Using Gaussian KDE methodology, densest points are determined for each z position, even if they do not appear to be physically accurate. Obviously, data points $z < -0.1$ and $z > 0.6$ are not within the velocity profile $c(z)$ to be determined. Data points in range of $z \approx 0.25$, on the other hand, are certainly part of velocity profile due to high data density. Selection of reliable MDPs to be included in reconstruction of velocity profile requires statistical proof. An algorithm for validating statistically reliable data points is introduced in the following chapter.

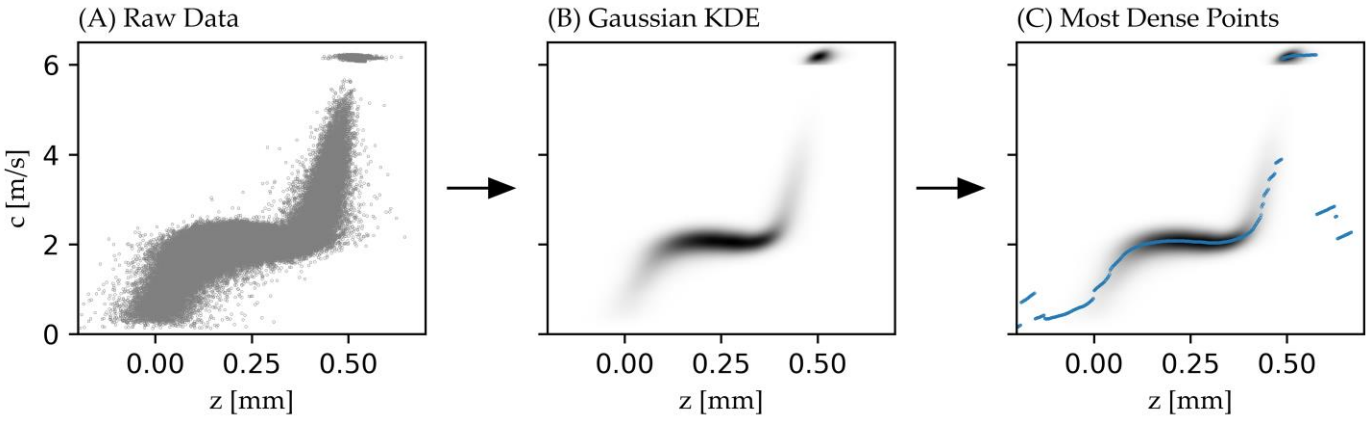

Fig. 6: (A) Raw data with high degree of variation in velocity data, (B) application of Gaussian Kernel Density Estimation to resolve density of sampled data, (C) collection of Most Dense Points (MDP) along z-coordinate.

2.4 Profile Validation Algorithm

In the following, a method is presented to statistically validate MDPs from Gaussian KDE and to decide whether an investigated MDP is to include in reconstruction of the velocity profile or is to be rejected. For this purpose, in a first step, a required accuracy with respect to localization of spatial coordinate z and associated velocity c is defined. In present case accuracy is specified to $\Delta z = 4\ \mu m$ and $\Delta c = 0.05\ m/s$, cf. Fig. 7 (A). In a next step, it is statistically proofed whether evaluated MDP is classified as valid by considering surrounding raw data with a confidence level of 99%. Since surrounding measurement data depends on the shape of the velocity profile, an algorithm searches for suitable values. For this purpose, ellipses are formed around examined MDP in a normalized representation of the raw data (Fig. 7 (B)). Ellipses are varied with respect to dimension of semi-axes and rotational orientation, allowing the surrounding data points to be statistically evaluated. A t-test is performed for the data points in each ellipse and a confidence interval (confidence level 99%) is calculated based on contained data points. If calculated confidence interval is less than or equal to the previously defined limits ($\Delta z = 4\ \mu m$, $\Delta c = 0.05\ m/s$), then examined MDP is declared valid and is included in reconstruction of the velocity profile. If confidence interval determined by the t-test falls outside defined limits, evaluated MDP is rejected and is not included in reconstruction. Fig. 7 (C) shows exemplary validated data sets around the corresponding MDPs. The reconstruction of the flow profile (Fig. 7 (D)) is accomplished by a least squares optimization.

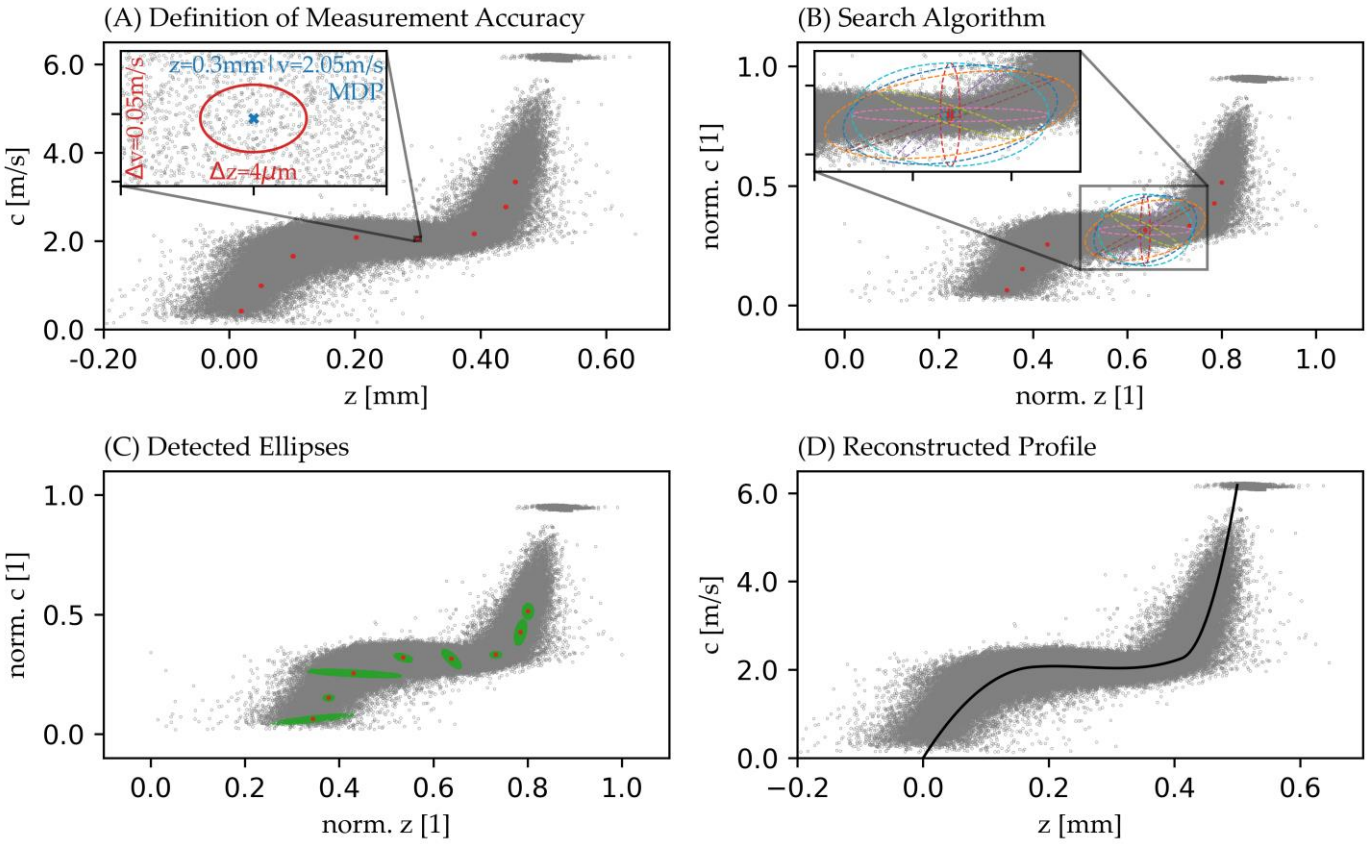

Fig. 7: (A) Definition of desired measurement accuracy for an investigated Most Dense Point (MDP) along z-Position, (B) Elliptical Search Algorithm to detect statistically relevant datapoints by variation of ellipse's semi-axes and tilting, (C) Visualization of detected valid ellipses for an investigated MDP, (D) Reconstructed velocity profile c(z) by usage of Least-Squares-Minimization. Displayed data is reduced both for Most Dense Points as well as examined ellipses for better vizualisation.

3 Results and Discussion

As described in Table 1, five radii as well as three rotational speeds are investigated resulting in a total of 15 different velocity profiles. Velocity profiles are depicted in Fig. 8 in following order: First three columns denote rotational speeds, fourth column compares all speeds in a normalized representation for comparative purposes where $u = R \cdot 2\pi n$ denotes disk's angular speed. First five rows represent radii arranged in decreasing order as they appear geometrically on the rotating disk. Last row contains normalized representations of determined velocity profiles for comparison of all radii where $w = 0.5\ mm$ represents gap width.

In Fig. 8 column one ($n = 1000\ rpm$) a mostly linear characteristic is observed with deviations from linear behavior near rotating disk. Further, development of a steeper velocity gradient at $z =$

$0.0\ mm$ is detected for $R = 20.0\ mm$. Both deviation from linearity as well as steeper velocity gradient indicate rotational speed being selected too high to achieve envisaged strictly linear velocity distribution. Normalized representation of velocity profiles (row 6, column 1) shows good agreement for normalized positions $z/w > 0.5$ and slight deviations for $z/w \leq 0.5$, thus underpinning rotational speed chosen too high. Result may be improved by decreasing rotational speed further, thus creating attempted strictly linear profile.

Analyzing Fig. 8 column two ($n = 1500rpm$), development of a pre-state solid body rotational core flow ($R = 20.0\ mm$, row 1, column 2) from mostly linear velocity distribution ($R = 10.0\ mm$, row 5, column 2) is observed. Normalized representation of velocity profiles (row 6, column 2) shows expected deviations between radii, thus illustrating change of profile shape depending on observed radius.

For $n = 3000\ rpm$ (Fig. 8, column 3) a fully developed solid body rotational core flow is recognized. Range of solid body core flow may be allocated to $\Delta z \approx 0.21\ mm$, starting at $z \approx 0.17\ mm$ and ending at $z \approx 0.38\ mm$, thus occupying about 42 % of total gap. Normalized representation of velocity profiles (row 6, column 3) shows good agreement between all radii. Solid body core flow rotates with a normalized speed of $c/u = 0.34$, which is slightly lower than reported in common literature (e.g., (Pfleiderer/Petermann, 2004) (Gülich, 2014)), where c/u is usually in range of 0.4 to 0.5. Determined drift to a lower quotient c/u may be attributed to drastically lower wall roughness of optical glass compared to commonly used materials in turbomachinery (e.g., stainless steel, cast steel, brass, various plastics).

4 Conclusions and Outlook

LDV Profile Sensor technology is suitable for locally resolving velocity profiles in a gap of $w = 0.5\ mm$. Thus, this technology has potential to provide needed validations of flow topologies in Ventricular Assist Devices. Evaluation of measurement data using Gaussian Kernel Density Estimation as well as developed Profile Validation Algorithm serve as solid tools to reliably determine velocity distributions. Presented feasibility study is deemed successful and employed LDV Profile Sensor technology may serve as new methodology to assist VAD development.

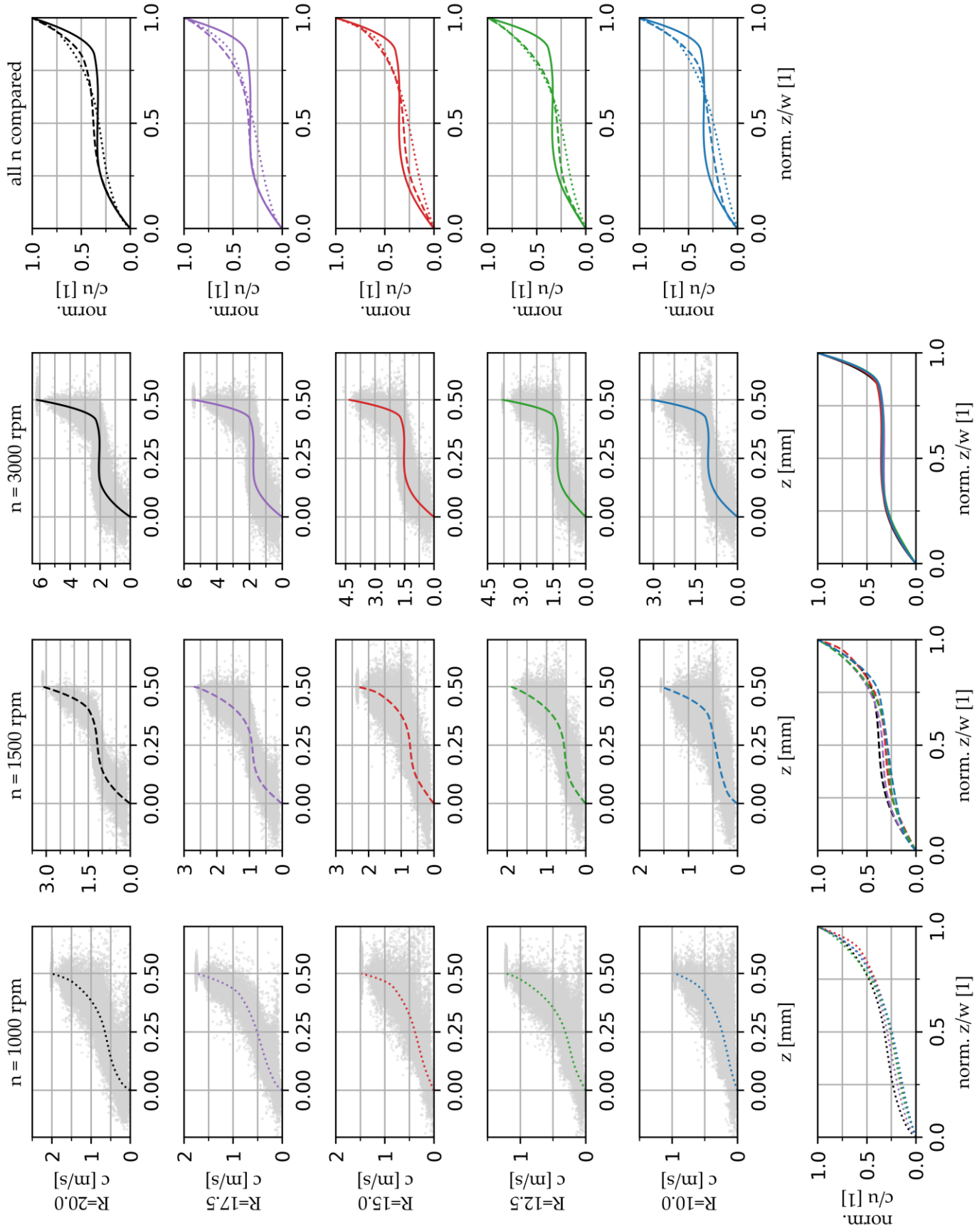

Fig. 8: Determined velocity profiles in comparision

References

Czarske, J., Büttner, L., Razik, T., & Müller, H. (2002). Boundary layer velocity measurements by a laser Doppler profile sensor with micrometre spatial resolution. Measurement Science and Technology, 13(12), 1979-1989 ,https://doi.org/10.1007/s00348-021-03148-0

Daily, J. W., and Nece, R. E. (March 1, 1960). "Chamber Dimension Effects on Induced Flow and Frictional Resistance of Enclosed Rotating Disks." ASME. J. Basic Eng. March 1960; 82(1): 217–230. https://doi.org/10.1115/1.3662532

Florjancic, S.: Annular seals of high energy centrifugal pumps: A new theory and full scale measurement of rotordynamic coefficients and hydraulic friction factors. Diss. ETH Zürich (1990)

Gülich, J. F., Kreiselpumpen, Handbuch für Entwicklung, Anlagenplanung und Betrieb, 4. Auflage, Berlin/Heidelberg: Springer Vieweg, 2014.

Haddadi, S., Poncet, S., "Turbulence Modeling of Torsional Couette Flows", International Journal of Rotating Machinery, vol. 2008, Article ID 635138, 27 pages, 2008. https://doi.org/10.1155/2008/635138

Hamkins, C.P.: The surface flow angle in rotating flow: Application to the centrifugal impeller side gap. Diss. TU Kaiserslautern, Shaker, Aachen (2000)

Kosyna, G., Lünzmann, H.: Experimental investigations on the influence of leakage flow in centrifugal

pumps with diagonal clearance gap. ImechE Paper C439/010 (1992)

Kriegseis, J., Mattern, P., Dues, M., Combined Planar PIV and LDV Profile-Sensor Measurements in a Rotor-Stator Disk Configuration, 18th International Symposium on the Application of Laser and Imaging Techniques to Fluid Mechanic LISBON PORTUGAL JULY 4 – 7, 2016

Lauer, J., et al.: Tip clearance sensitivity of centrifugal pumps with semi-open impellers. ASME Paper FEDSM97-3366 (1997)

Launder, B., Poncet, S., and Serre, E., Laminar, Transitional, and Turbulent Flows in Rotor-Stator Cavities, Annual Review of Fluid Mechanics, Vol. 42:229-248 (Volume publication date 1 January 2010), First published online as a Review in Advance on August 25, 2009, https://doi.org/10.1146/annurev-fluid-121108-145514

Pfleiderer, C., Petermann, H., Strömungsmaschinen, 7. Auflage, Berlin/Heidelberg: Springer, 2004.

Schubert, F. (1988). Untersuchungen der Druck- und Geschwindigkeitsverteilung in Radseitenräumen radialer Strömungsmaschinen (Doctoral Dissertation, Technische Universität Carolo-Wilhelmina zu Braunschweig).

Schüle, C.Y., Thamsen, B., Blümel, B., Lommel, M., Karakaya, T., Paschereit, C.O., Affeld, K. and Kertzscher, U. (2016), Experimental and Numerical Investigation of an Axial Rotary Blood Pump. Artificial Organs, 40: E192-E202. https://doi.org/10.1111/aor.12725

Schüle CY, Affeld K, Kossatz M, Paschereit CO, Kertzscher U. Turbulence Measurements in an Axial Rotary Blood Pump with Laser Doppler Velocimetry. The International Journal of Artificial Organs. 2017;40(3):109-117. doi:10.5301/ijao.5000571

SciPy Documentation, The SciPy community, scipy.stats.gaussian_kde, 2022, https://docs.scipy.org/doc/scipy/reference/generated/scipy.stats.gaussian_kde.html , Last Online Access 21.05.2022

Schultz-Grunow, F. (1935), Der Reibungswiderstand rotierender Scheiben in Gehäusen. Z. angew. Math. Mech., 15: 191-204. https://doi.org/10.1002/zamm.19350150403

Strauch, C., Thamsen, P.U., Escher, A., & Granegger, M. "Experimental Hydraulic and Mechanical Characterisation of a Double-Flow Implantable Blood Pump." Proceedings of the ASME 2020 Fluids Engineering Division Summer Meeting collocated with the ASME 2020 Heat Transfer Summer Conference and the ASME 2020 18th International Conference on Nanochannels, Microchannels, and Minichannels. Volume 2: Fluid Mechanics; Multiphase Flows. Virtual, Online. July 13–15, 2020. V002T03A016. ASME. https://doi.org/10.1115/FEDSM2020-20248

Strauch, C., Experimentelle Untersuchung der hydraulischen Verlustleistung von Herzunterstützungs-pumpen, TU Berlin, Dissertation, ISBN 978-3-96729-142-1

Strauch, C., Peter, J., Thamsen, P.U., " Methodology for Experimental Investigation of Hydraulic and Mechanical Characteristics of Ventricular Assist Devices", Accepted for publication in Proceedings of the ASME 2022 Fluids Engineering Division Summer Meeting. August 3–5, 2022, Toronto, Ontario, Canada

Thamsen B, Gülan U, Wiegmann L, Loosli C, Schmid Daners M, Kurtcuoglu V, Holzner M, Meboldt M. Assessment of the Flow Field in the HeartMate 3 Using Three-Dimensional Particle Tracking Velocimetry and Comparison to Computational Fluid Dynamics. ASAIO J. 2020 Feb;66(2):173-182. doi: 10.1097/MAT.0000000000000987. PMID: 30883404.